

Phase behavior and molecular self-assembly of some calamitic/bent-core nematic mixtures

M. Cvetinovic, M. Stojanovic, D. Obadovic, I. Ristic, A. Vajda, K. Fodor-Csorba & N. Eber

To cite this article: M. Cvetinovic, M. Stojanovic, D. Obadovic, I. Ristic, A. Vajda, K. Fodor-Csorba & N. Eber (2016) Phase behavior and molecular self-assembly of some calamitic/bent-core nematic mixtures, *Molecular Crystals and Liquid Crystals*, 630:1, 28-36, DOI: 10.1080/15421406.2016.1146863

To link to this article: <http://dx.doi.org/10.1080/15421406.2016.1146863>



Published online: 01 Jul 2016.



Submit your article to this journal [↗](#)



Article views: 3



View related articles [↗](#)



View Crossmark data [↗](#)

Phase behavior and molecular self-assembly of some calamitic/bent-core nematic mixtures

M. Cvetinov^a, M. Stojanovic^a, D. Obadovic^b, I. Ristic^c, A. Vajda^d, K. Fodor-Csorba^d, and N. Eber^d

^aDepartment of Physics, University of Novi Sad, Novi Sad, Serbia; ^bFaculty of Education, University of Novi Sad, Sombor, Serbia; ^cFaculty of Technology, University of Novi Sad, Novi Sad, Serbia; ^dInstitute for Solid State Physics and Optics, Wigner Research Centre for Physics of Hungarian Academy of Sciences, Budapest, Hungary

ABSTRACT

The primary research goal within contemporary liquid crystalline display industry is to discover new materials exhibiting phase temperature range and properties useful for display application. In this work, we studied five binary mixtures composed of different concentrations of bent-core and calamitic compounds. Pure compounds and selected mixtures were studied by polarizing optical microscopy, differential scanning calorimetry, and X-ray diffractometry, as well as by semi-empirical quantum-chemical calculations. Phase transition types, temperatures, and enthalpies were determined. Molecular packaging in the nematic mesophase is proposed. All studied mixtures exhibit the nematic phase of wide temperature range near to the room temperature.

KEYWORDS

Bent-core; calamitic; liquid crystals; nematic; phase transitions

Introduction

For liquid crystalline displays industry, temperature range and properties of the applied mesophase are of paramount importance. Notwithstanding the fact that materials exhibiting required characteristics could be synthesized *de novo* [1–4], this is slow and expensive process. Therefore, such materials are most often multicomponent mixtures, composed of diversely shaped molecular constituents [5–9].

The cornerstone of the industry is the nematic phase due to its use in super-twisted nematic, in-plane switching and vertical alignment technologies [10]. Broad temperature range of the nematic phase and the absence of low-temperature smectic or the columnar phase is of utmost importance for nematic liquid-crystalline display construction [11].

Importance of bent-core liquid crystals was first attributed to their unconventional smectic phases possessing spontaneous electric polarization [12,13]. Yet, focus of scientific interest shifted to pursuit of bent-core nematics, BCN, expressing the elusive biaxial nematic phase. If discovered unequivocally, phase biaxiality would lead to dramatic improvement in performance of standard nematic liquid crystalline displays. Additional peculiarity of BCN is the existence of stable layered clusters, where nematic order exists only on a length scale much larger than the size of clusters [14,15]. Inheritance of this cybotactic nematic phase is evident

CONTACT M. Cvetinov  miroslav.cvetinov@df.uns.ac.rs  Department of Physics, University of Novi Sad, Trg Dositeja Obradovica 4, Novi Sad, Serbia.

Color versions of one or more of the figures in the article can be found online at www.tandfonline.com/gmcl.

© 2016 Taylor & Francis Group, LLC

even in binary mixture with calamitic compounds [16]. Nonetheless, commercial application of BCN proved to be difficult due to the high temperature range of their nematic phase [17,18].

In order to obtain the nematic phase with wide temperature range close to the room temperature we prepared and studied five binary mixtures composed of different concentrations of bent-core and calamitic compounds. Although selected components possess ester linkages in their rigid cores and terminal chains of comparable lengths, they differ greatly in molecular shape and dimensions.

Materials and methods

Shown in Figs. 1 and Fig. 2 are bent-core compound 4,6-dichloro-1,3-phenylene bis [4'-(10-undecen-1-yloxy)-1, 1'-biphenyl-4-carboxylate] (I) and calamitic compound 4-propylox yphenyl 4'-dodecyloxybenzoate (II). While calamitic compound belongs to the long known and huge family of prototypical calamitic liquid crystals: 4'-alkyl/alkoxyphenylbenzoates [6,19], selected bent-core compound is comparatively recent [20].

Phase transition behavior was investigated using a DuPont DSC 910. Hermetically sealed aluminum pans containing 1–3 mg of sample were prepared. Calibration of the equipment was carried out by indium as temperature standard. All samples were melted at 120°C, to ensure complete melting and resetting the thermal history, and cooled at room temperature for 2 days. The nonisothermal analyses were performed with heating rate 10°C min⁻¹ from 20 to 150°C, well within the limit of thermal stability [21]. Subsequently, sample was allowed to cool spontaneously to the room temperature, thus only T_{I-N} phase temperatures could be determined unambiguously from DSC in cooling.

The presence and identification of the potential mesophases was achieved from the characteristic textures and their changes observed in a polarizing optical microscope (POM) Carl Zeiss Jena on nonoriented samples. Hot-stage with platinum–rhodium thermocouple was employed for controlled heating and cooling of the sample. Cell thickness of 100 μm was achieved using mylar spacers that separated glass substrates. Clamped together, cell was filled by capillary action with studied sample.

In order to obtain more structural information and with intention to affirm or refute previously reported sequences of phases, nonoriented samples were investigated by X-ray diffraction in Bragg–Brentano $\theta:2\theta$ geometry using a conventional powder diffractometer, Seifert V-14, equipped with an automated high-temperature kit Paar HTK-10. Diffraction was detected at the CuK α radiation of 0.154059 nm, with Ni filter installed and in the absence of monochromator. Calibration was performed employing two most intense platinum lines. Continual scan was employed with scanning speed of 1 °2 θ min⁻¹.

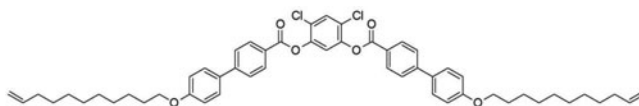


Figure 1. Structural formula of compound I.

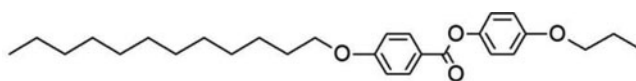


Figure 2. Structural formula of compound II.

Table 1. Temperatures (°C) and enthalpies (J/g) of mesophase transitions for compounds under the study obtained by DSC and POM in heating (Cr–crystalline, SmA–smectic A, N–nematic, I–isotropic phase).

Code	Mol%I	m_{mol} [Da]	Cr ₁	T[°C]	Cr ₂	T[°C]	SmA	T[°C]	N	T[°C]	I
II	0	440.62	•	66.5 [101.0]			•	80.0 [*]	•	82.5 [4.5]	•
Mix1	11.2	489.38	•	39.5 [86.0]	•	49.5 [59.7]			•	73.5 [1.2]	•
Mix2	25.1	549.90	•	39.5 [28.8]	•	45.5 [83.4]			•	70.5 [3.7]	•
Mix3	33.5	586.72	•	38.5 [26.0]	•	44.5 [99.0]			•	75.0 [1.3]	•
Mix4	43.0	627.82	•	39.0 [17.4]	•	46.0 [82.8]			•	79.5 [3.6]	•
Mix5	66.8	731.43	•	67.0 [33.0]					•	87.5 [4.0]	•
I	100	875.97	•	77.5 [58.7]					•	104.9 [1.4]	•

Note: *The intensity of the DSC peak is comparable with the sensitivity; reliable enthalpy data are not available

As a means to properly represent molecular packaging in mixtures, the semiempirical method of quantum chemistry (RM1) was employed to determine minimum energy conformations of the molecules and to calculate their electrostatic potential maps.

Results and discussion

The goal of the present work was to test the miscibility of the bent-core compound **I** with the calamitic compound **II**, and to investigate the mesomorphic behavior of their binary mixtures. For the detailed study, five mixtures, **Mix1** to **Mix5**, have been prepared with 20, 40, 50, 60, and 80 wt% (11.2, 25.1, 33.5, 43.0, and 66.8 mol%) of the bent-core compound **I**, respectively. Molar percentages, molar masses, and phase transition temperatures of the studied compounds evaluated from the DSC curves are summarized in **Tables 1** and **2** for heating and cooling, respectively. Mixtures under investigation were stable, showing no signs of segregation after one month storage period.

Analysis of thermal behavior of mixtures was performed with regard to the heating cycle for the reason that fast cooling rate caused supercooling of mesophases. Obvious finding is disappearance of the smectic phase in all investigated mixtures. The nematic phase closest to the room temperature (44.5°C) is found in **Mix3**. Moreover, the temperature range of its nematic phase (30.5°C) is wider than in starting bent-core compound **I** (27.4°C). Evident by two DSC peaks of high enthalpy values, polymorphism of crystalline phases is expressed in **Mix1–Mix4** in heating. Both melting and clearing point temperatures were lowered in mixtures **Mix1–Mix4** with respect to pure compounds.

Figs. 3 and **4** show representative DSC curves for all mixtures and pure compounds obtained in a first cooling and second heating cycle, respectively. In heating, all phase transition temperatures were determined by DSC and subsequently marked with arrows. In the cooling cycle, because of its spontaneity, only the isotropic–nematic phase transition temperature was detected by DSC; other transition temperatures were detected by POM.

Table 2. Temperatures of mesophase transitions (°C) for compounds under the study obtained by DSC and POM in cooling.

Code	Mol%I	m_{mol} (Da)	Cr ₁	T(°C)	SmA	T(°C)	N	T[°C]	I
II	0	440.62	•	65.0	•	79.5	•	81.0	•
Mix 1	11.2	489.38	•	48.0			•	70.5	•
Mix 2	25.1	549.90	•	43.0			•	68.5	•
Mix 3	33.5	586.72	•	42.0			•	73.0	•
Mix 4	43.0	627.82	•	44.0			•	76.5	•
Mix 5	66.8	731.43	•	56.0			•	85.0	•
I	100	875.97	•	60.9			•	102.7	•

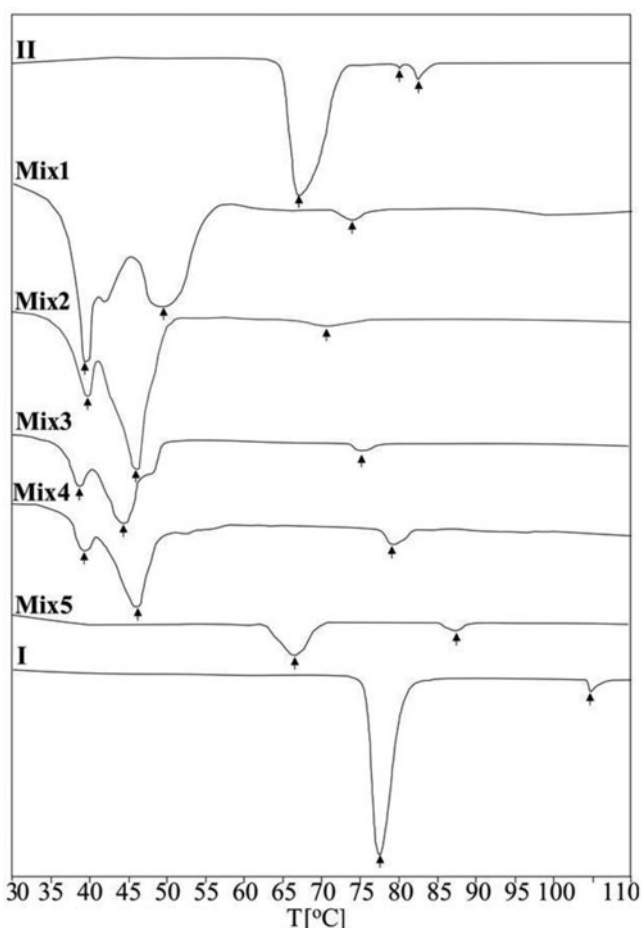


Figure 3. DSC curves for pure compounds and their binary mixtures obtained in heating.

Microphotographs of some characteristic textures of the various mesophases obtained in cooling of unoriented planar samples are presented in Fig. 5. Textures obtained in heating are similar to textures obtained in cooling. Nematic phases are characterized by observation of schlieren textures (Figs. 5(b) and (c)) and thread-like textures (Figs. 5(a) and (d)) which are the result of nonuniform alignment of nematic molecules [22].

All prepared binary mixtures and pure compounds were investigated by X-ray diffraction. Selected diffractograms are presented in Fig. 6. Molecular packaging parameters, namely thickness of smectic layers d (if layer exists) and mean lateral intermolecular distance D , were determined and shown in Table 3 [23–25]. These parameters were determined from positions of low- and high-angle reflections, respectively. Calculation was performed using Bragg's law: $n\lambda = 2d\sin\theta$. Albeit second-order reflections ($n = 2$) exist on some diffractograms, they were not shown in Table 3. Zero shift and sample displacement errors were incorporated in the tabular data.

The isotropic–nematic phase transition is characterized by right shift of diffuse reflection at high Bragg angle. This shift implies lessening of the lateral distance between molecules and subsequently denser packing of molecules in the nematic phase.

Smectic SmA phase of pure compound II is characterized by low angle diffraction peak at $3.1^\circ 2\theta$, thus indicating interplanar distance of 2.84 nm. This distance is slightly shorter than

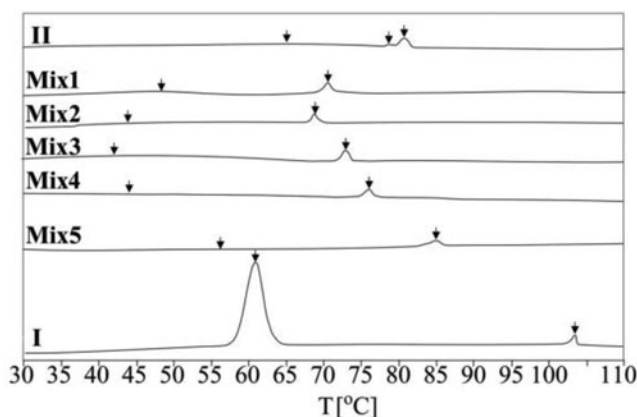


Figure 4. DSC curves for pure compounds and their binary mixtures obtained in cooling.

effective molecular length, which imply either slight unbiased tilt due to thermal rotation of molecules or existence of some gauche defects in terminal alkyl chains [26]. Due to similar values of molecular length and layer spacing, existence of the interdigitated smectic phase is ruled out [27].

Subsequent cooling leads to crystallization of the sample, evident by large number of reflections. The absence of amorphous halo and high sharpness of diffraction peaks suggest good crystallinity of the sample. In contrast to compound **II**, **Mix2** exhibits much lower crystallinity due to considerable difference between molecular shapes of starting compounds. The absence of smectic phases stems from this difference; bulky and rigid bent-core molecules hinder the formation of smectic layers.

Molecular models were calculated to clarify molecular self-assembly in mesophase. Owing to large number of nonhydrogen atoms in studied molecules, computationally light semi-empirical methods are often utilized to calculate molecular parameters [28,29]. Among them, RM1 method yields minor average errors for both bond lengths and bond angles [30].

Table 3. Molecular parameters of the investigated mixtures for all observed phases at a fixed temperature T (°C): angles corresponding to the reflection peaks 2θ (°), effective layer thickness d (in nm; error of measurements was $\sigma d \approx 0.001$ nm), average repeat distance D (in nm; error of measurements was $\sigma D \approx 0.002$ nm).

Sample	T (°C)	2θ (°)	d (nm)	D (nm)
II	90 (I)	18.6	2.848	0.477
	80(N)	18.8		0.472
	67 (SmA)	3.1		
		19.7		0.450
Mix 1	80(I)	18.8	0.472	
	60(N)	20.0	0.444	
Mix 2	93(I)	18.4	0.481	
	67(N)	19.4	0.457	
Mix 3	93(I)	17.8	0.497	
	63(N)	19.0	0.466	
Mix 4	95(I)	18.7	0.474	
	70(N)	19.3	0.459	
Mix 5	100(I)	19.3	0.459	
	75(N)	19.8	0.448	
I	110(I)	19.3	0.459	
	90(N)	20.0	0.444	

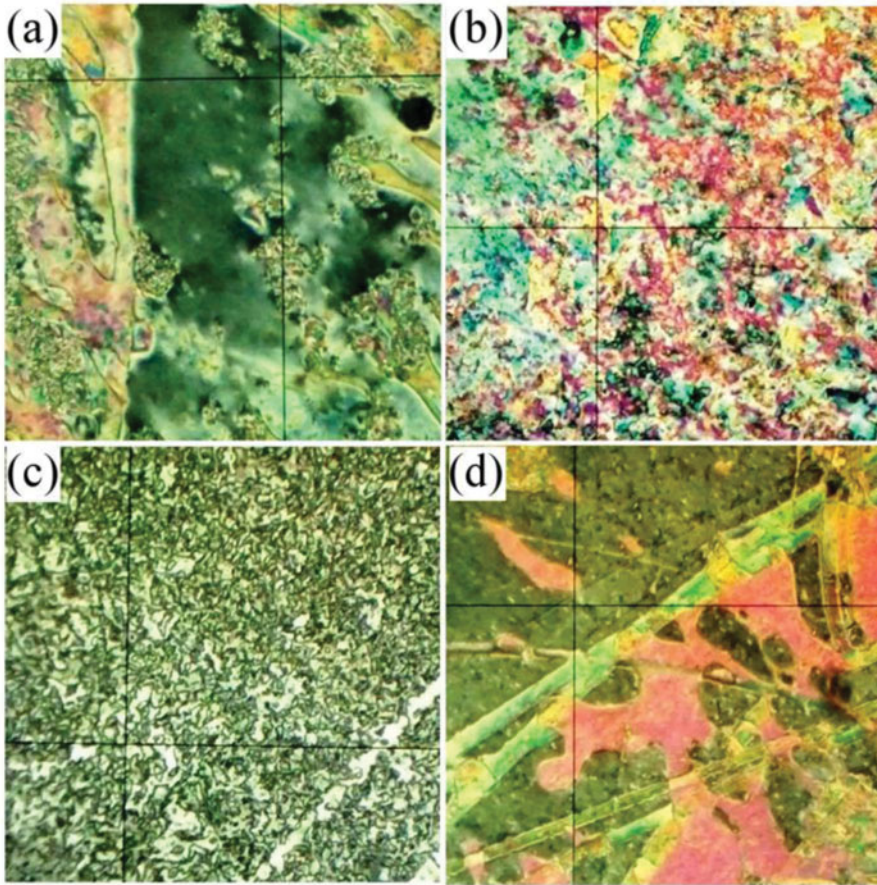


Figure 5. Micrographs of nematic phases of unoriented samples of: (a) **Mix1** at 65°C, (b) **Mix3** at 70°C, (c) **Mix4** at 58°C, and (d) **Mix5** at 78°C, obtained on POM in cooling. All micrographs are 300 μm wide.

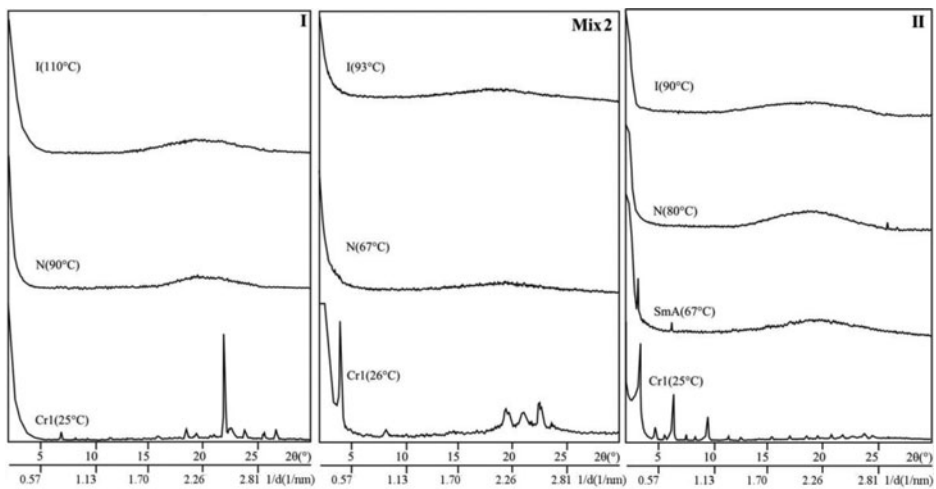


Figure 6. X-Ray diffractograms of unoriented samples of: Compound **I**, **Mix2**, and compound **II**.

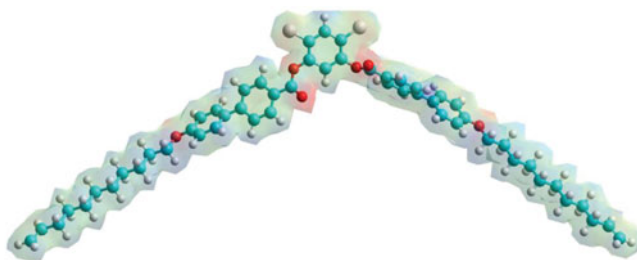


Figure 7. Electrostatic potential map of the minimum energy conformation of compound **I**.

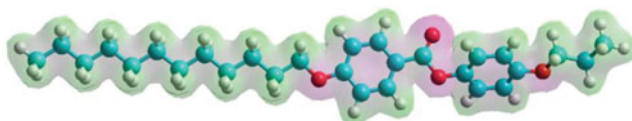


Figure 8. Electrostatic potential map of the minimum energy conformation of compound **II**.

The electrostatic potential map of compound **I** is shown in [Fig. 7](#). The calculated bending angle between the two arms of the molecule is 121.32° . The angle between the two neighboring phenyl rings in both arms of the molecule is 44.1° . Molecular length of compound is 4.65 nm. The linear length of the half of its rigid molecular core is 1.40 nm and the linear length of each alkyl chain is 1.44 nm.

The electrostatic potential map of compound **II** is shown in [Fig. 8](#). Total length of the compound is 2.97 nm, while calculated torsion angle between biphenyl rings is 53.9° . In fully extended conformation, alkyl chains have length of 1.38 nm and 0.25 nm, respectively. Value of computed molecular length is in agreement with the X-ray measurements.

Modeling of molecular packaging in mesophases relies on the determination of molecular shapes. For molar concentrations of 25.1 mol% of compound **I** in **Mix2**, assumed molecular packaging is shown in [Fig. 9](#). Fully extended conformation of flexible alkyl chains is the most probable one at low temperatures. Uniform orientation of calamitic molecules is thwarted by

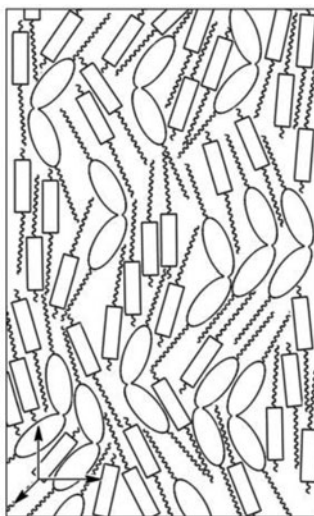


Figure 9. Assumed molecular packing in nematic phase of **Mix2**.

inflexible bent-core molecules. Calamitic molecules are oriented parallel to either one molecular arm of bent-core molecules or another. Nonpolar order of molecules is preserved, hence there is equal probability of molecules pointing in any of two possible directions (up and down, or left and right). Determination of existence of cybotactic groups in the nematic phase of mixtures would exceed scope of this article, hence it was not performed.

Conclusion

The present study was performed with the intention to elucidate influence of mixing bent-core and rod-like molecules on mesomorphic properties. Based on POM, DSC, and X-ray measurements on several mixtures, we have found that the polymorphism of the pure calamitic component **II** is not preserved in any mixture. The nematic phase remains detectable in all studied mixtures. Compared to the starting compounds, **Mix3** has its temperature range of the nematic phase broadened ($\Delta T_N = 30.5^\circ\text{C}$) and shifted closer to the room temperature ($T_{Cr-N} = 44.5^\circ\text{C}$). Together with disappearance of the smectic phase, this result suggests that combining conventional calamitics with bent-core mesogens with an appropriate molecular design may yield mixtures valuable for industry of nematic liquid crystalline displays.

Acknowledgments

This work was partly supported by the research Grant No. OI171015 from the Ministry of Education and Science of the Republic of Serbia and the Hungarian Research Fund OTKA K81250.

References

- [1] Hu, J.S., Liu, X. F., Meng, Q. B., & Zhang, Y. (2014). *J. Mater. Sci.*, *49*, 1229.
- [2] Stojanović, M., Bubnov, A., Obadović, D. Ž., Hamplová, V., Cvetinov, M., & Kašpar, M. (2014). *Mater. Chem. Phys.*, *146*, 18.
- [3] Karim, M. R., Sheikh, M. R. K., Salleh, N. M., Yahya, R., Hassan, A., & Hoque, M. A. (2013). *Mater. Chem. Phys.*, *140*, 543.
- [4] Eran, B. B., Nesrullajev, A., & Canli, N. Y. (2008). *Mater. Chem. Phys.*, *111*, 555.
- [5] Cvetinov, M., Obadović, D., Stojanović, M., Lazar, D., Vajda, A., Éber, N., et al. (2013). *Liq. Cryst.*, *40*, 1512.
- [6] Kumar, S. (2001). *Liquid Crystals: Experimental Study of Physical Properties and Phase Transitions*, Cambridge University Press: Cambridge.
- [7] Lapanik, V., Bezborodov, V., Sasnouski, G., & Haase, W. (2012). *Phase Transit.*, *85*, 900.
- [8] Obadović, D. Ž., Stojanović, M., Jovanović-Šanta, S., Cvetinov, M., Lazar, D., et al. (2011). *Mol. Cryst. Liq. Cryst.*, *547*, 46 [1736].
- [9] Cvetinov, M., Obadovic, D. Z., Stojanovic, M., Vajda, A., Fodor-Csorba, K., et al. (2014). *Chinese Phys. B*, *23*, 096402.
- [10] den Boer, W. (2011). *Active Matrix Liquid Crystal Displays: Fundamentals and Applications*, Elsevier Science, Oxford, UK.
- [11] Keith, C., Lehmann, A., Baumeister, U., Prehm, M., & Tschierske, C. (2010). *Soft Matter*, *6*, 1704.
- [12] Takezoe, H., & Takanishi, Y. (2006). *Jpn. J. Appl. Phys.*, *45*, 597.
- [13] Vijay Srinivasan, M., Kannan, P., & Roy, A. (2013). *J. Mater. Sci.*, *48*, 2433.
- [14] Francescangeli, O., Vita, F., & Samulski, E. T. (2014). *Soft Matter*, *10*, 7685.
- [15] Jákli, A. (2013). *Liq. Cryst. Rev.*, *1*, 65.
- [16] Hong, S. H., Verdúzco, R., Gleeson, J. T., Sprunt, S., & Jákli, A. (2011). *Phys. Rev. E.*, *83*, 061702.
- [17] Gleeson, H. F., Kaur, S., Görtz, V., Belaisaoui, A., Cowling, S. et al. (2014). *Chem. Phys. Chem.*, *15*, 1251.
- [18] Nair, G. G., Bailey, C. A., Taushanoff, S., Fodor-Csorba, K., Vajda, A., et al. (2008). *Adv. Mater.*, *20*, 3138.

- [19] Blair, T. T., Neubert, M. E., Tsai, M., & Tsai, C.C. (1991). *J. Phys. & Chem. Ref. Data.*, 20, 189.
- [20] Fodor-Csorba, K., Vajda, A., Jakli, A., Slugovc, C., Trimmel, G., et al. (2004). *J. Mater. Chem.*, 14, 2499.
- [21] Beica, T., Zgura, I., Frunza, L., Ganea, P., Frunza, S., et al. (2011). *Romanian Rep. Phys.*, 63, 741.
- [22] Nesrullajev, A., & Avci, N. (2011). *Mater. Chem. & Phys.*, 131, 455.
- [23] Weissflog, W., Shreenivasa Murthy, H. N., Diele, S., & Pelzl, G. (2006). *Philos. l T. Roy. Soc. Math. l, Phys. Eng. Sci.*, 364, 2657.
- [24] Schröder, M. W., Diele, S., Pelzl, G., Pancenko, N., & Weissflog, W. (2002). *Liq. Cryst.*, 29, 1039.
- [25] Takanishi, Y., Shin, G. J., Jung, J. C., Choi, S.W., Ishikawa, K., et al. (2005). *J. Mater. Chem.*, 15, 4020.
- [26] Suryanarayanan, C., Prasannan, A., Hong, P.D., Sambathkumar, B., & Somanathan, N. (2014). *Mater. Chem. Phys.*, 143, 1352.
- [27] Ungar, G., Noble, K., Percec, V., & Johansson, G. (2000). *J. Mater. Sci.*, 35, 5241.
- [28] Tiwari, S. N. (2006). *Prog. Cryst. Grow. Ch. Mater.*, 52, 150.
- [29] Mishra, M., Dwivedi, M. K., Shukla, R., & Tiwari, S. N. (2006). *Prog. Cryst. Grow. Ch. Mater.*, 52, 114.
- [30] Rocha, G. B., Freire, R. O., Simas, A. M., & Stewart, J. J. P. (2006). *J. Comp. l Chem.*, 27, 1101.